SAPIENZA
UNIVERSITA' DI ROMA

DOTTORATO DI RICERCA IN MEDICINA SPERIMENTALE
XXIX CICLO

"USPIO-labeling nei macrofagi M1 e M2: studio in vitro con risonanza magnetica"

DOTTORANDO
Dottoressa Chiara Zini

DOCENTE GUIDA
Prof. Andrea Laghi

COORDINATORE DEL DOTTORATO
Prof.ssa Maria Rosaria Torrisi

ANNO ACCADEMICO 2015-2016

INTRODUCTION

Background

Pre-clinical and clinical investigations have shown that pro-inflammatory leukocytes regulate the development and progression of a large variety of cancers, including lung, breast, colon, prostate, cervical, liver, ovarian, lymphoma and thyroid cancers and some pediatric solid malignancies [1-4].

Tumor-associated macrophages (TAM) play a key role in this process [5-9]. They secrete growth factors that support the proliferation of neoplastic cells, along with delivering vascular endothelial growth factor (VEGF) to activate tumor angiogenesis [6] and produce cytokines and extracellular proteases to support tumor invasion and metastasis [8].

TAM originate from circulating monocytes which are recruited to the tumor site and programmed by tumor-derived factors such as colony-stimulating factor-1 (CSF-1), vascular endothelial growth factor A (VEGF-A) and CC chemokine ligand 2 (CCL2) [10-11]. These and other factors in the tumor microenvironment shape the TAM phenotype and skew them toward tumor-supportive M2-polarized macrophages, although M1-polarized TAM with anti-tumor activity were also reported in several types of cancer [12-15].

Tumor supporting functions of TAM includes the stimulation of tumor cell growth and the creation of favorable conditions for tumor cell intravasation into vessels and metastatic spread.

There is a growing set of evidence that specific subpopulations of TIE2 receptor expressing monocytes (TEM) in mice and humans significantly contribute to tumor angiogenesis [16-19]. These monocytes/macrophages are attracted into the tumors by endothelial cell (EC)-derived cytokine angiopoietin-2 (ANG-2), which interacts with its receptor TIE2 [20]. These cells had a signature of M2-polarized macrophages and expressed a panel of

markers including CD163, IL-10 and macrophage scavenger receptor-1 (MSR-1). Recently it was demonstrated that macrophages generated from CD16-positive monocytes (isolated by no-touch procedures) maintain a differential expression pattern and show higher phagocytosis activity when compared with macrophages, which were derived from the classical monocytes (CD14-positive) [21].

A recent immunological analysis revealed that TIE2(+)/CD31(+) macrophages constitute the predominant population of TAMs that infiltrate metastatic lymph nodes, distinct from tissue or inflammatory macrophages [22]. Importantly, these TIE2(+)/CD31(+) macrophages also heavily infiltrated metastatic lymph nodes from human breast cancer biopsies but not reactive hyperplastic lymph nodes. Thus, TIE2(+)/ CD31(+) macrophages may be a unique histopathological biomarker for detecting metastasis in clinical diagnosis, and a novel and promising target for TAM-specific cancer therapy.

Thus, it becomes increasingly important to identify patients whose tumors are heavily infiltrated by TEM/TAM, in order to stratify these patients to TEM/TAM depleting therapies and to monitor response to these new therapies.

To serve this goal, a noninvasive and easily repeatable imaging test would be advantageous over invasive biopsy.

The development of tumor specific imaging agents is highly desirable, as they may provide earlier and more accurate diagnosis, improve the assessment of the biological aggressiveness of the evaluated tumors, stratify patients basing on their immunoresponse and monitor treatment.

Cellular Imaging with USPIO MRI

In the era of personalized medicine, where drug delivery is a key issue, cell tracking would have a main role.

Cell tracking is extremely challenging and a standard method is no currently available: bioluminescence [23-24], radioisotopes [25-27] and Magnetic Resonance Imaging (MRI) [24, 1, 2] are among the most used techniques.

MRI has some inherent interesting characteristics: it combines high-spatial resolution with excellent soft tissue contrast while avoiding ionizing radiation.

A MRI contrast agent, consisting of a suspension of ferric ultrasmall superparamagnetic iron oxide particles (USPIO), has demonstrated a superparamagnetism resulting in T1, T2 and T2* shortening effects, similar to any other MR contrast agent; however, the carbohydrate shell results in a prolonged intravascular half life (1-2 days).

After injection the carbohydrate shell of the complex isolates the bioactive iron oxide core from plasma components until the whole iron-carbohydrate complex is taken up by reticuloendothelial system (RES) macrophages of the liver, spleen and bone marrow via phagocytosis within 24-36 hours [23-26].

This macrophage-dependent accumulation within the RES has been exploited to more accurately characterize both primary malignancies and metastatic disease [27].

Laghi et coll. previously reported that significant T2-effects in tumors on delayed MR images, acquired at 24 h post-contrast, corresponded to USPIO uptake and retention by TAM as revealed by immunohistopathology [25].

However, little is known regarding the association between macrophage polarization and USPIOs accumulation. Therefore, the aim of the present study was to evaluate if there are any differences in USPIO labeling for different macrophage populations.

Research Project

The aim of the present study was to evaluate if there are any differences in USPIO labeling for different macrophage populations.

- The primary objective of this study is the evaluation in vitro of P904 interaction with different macrophagic population (THP-1 cells M1/M2 polarizated and incubated with P904) using a 3T clinical scan; the light microscopy and the transmission electric microscopy were considered the gold standard.
- Second, the same MRI protocol has been used for the evaluation of P904 interaction with different macrophagic population (M1/M2 polarizated from healthy volunteer and from patient with cholangiocarcinoma).

MATERIALS & METHOD

TPH-1 Cell differentiation

Human Monocyte/Macrophage THP-1 cells (ATCC TIB-202) were maintained in culture in RPMI 1640 culture medium (Invitrogen) containing 10% of heat inactivated fetal bovine serum (Invitrogen) and supplemented with 10 mM Hepes (Gibco, #15630-056), 1 mM pyruvate (Gibco, #11360-039), 2.5 g/l D-glucose (Merck) and 50 pM ß-mercaptoethanol (Gibco; 31350–010). THP-1 monocytes were differentiated into macrophages using 320 nM of phorbol 12-myristate 13-acetate, PMA (Sigma), and polarized according to the modified method of Tjiu [26].

In order to obtain M1 polarization, cells were treated with PMA for 6 hours and then cultured with PMA plus LPS (10 ng/mL, Sigma) and IFN-γ (20 ng/mL, R&D System) for another 24 hours; for M2 polarization, cells were treated with PMA for 6 hours and then cultured with PMA plus IL-4 (20 ng/mL, R&D System) and IL-13 (20 ng/mL, R&D System) for another 24 hours. The control population of macrophages, which received no stimuli, were differentiated from THP-1 cells with 48 hours of incubation using PMA.

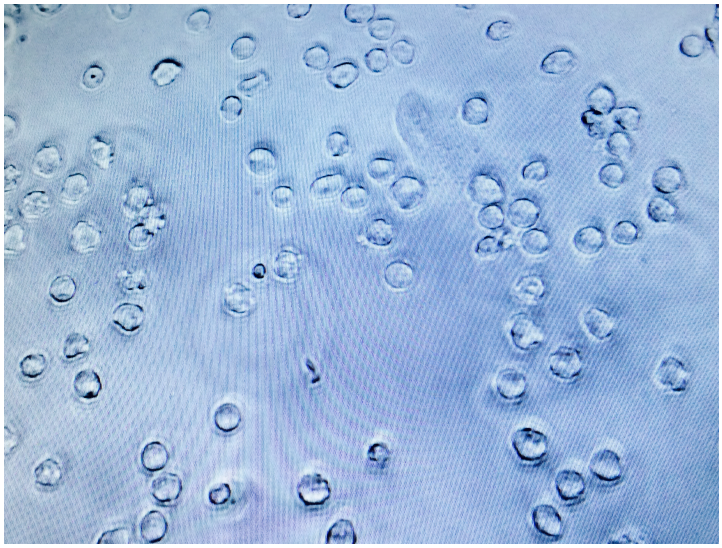

Fig.1 TPH-1 cells with 48 hours of incubation using PMA

RT-qPCR

After differentiation, total RNA was extracted using the RNeasy mini kit and DNase protocol (Qiagen). mRNA contained in 2 µg total RNA was reverse transcribed using a High Capacity RNA-to-cDNA kit (Applied Biosystems). Amplification reaction assays contained SYBRGreen PCR Master Mix (Applied Biosystem), primers iNOS (NM_010927, Forward: TTCTGTGCTGTCCCAGTGAG; Reverse: TGAAGAAAACCCCTTGTGCT) and Mcr1 (NM_008625, Forward: ATATATAAACAAGAATGGTGGGCAGT; Reverse: TCCATCCAAATGAATTTCTTATCC). RPS9 (40S ribosomal protein S9) was used as the reference gene for normalization, and mRNA abundance was quantified using the threshold cycle method. Quantitative PCR assay was performed on an ABI 7500 Fast Real-Time PCR System. All PCR reactions were performed in triplicate for this target gene and the internal control.

Relative gene expressions were presented with the -2ΔΔCt method.

Human Cell Differentiation

Peripheral blood (PB) was obtained from healthy volunteers and from patient with cholangiocarcinoma, following informed consent.

Total leukocytes were analyzed after lysis of erythrocytes using ammonium chloride. Peripheral blood mononuclear cells (PBMCs) were isolated using Ficoll-Hypaque gradient [17].

Subsequently the monocyte subsets classical, intermediate and nonclassical monocytes were gated based on their surface expression pattern [17]:

- CD14 + (LPS receptor) and CD16 - (FC III receptor) monocytes that mediate inflammatory responses called “inflammatory” monocytes

- CD14+ (LPS receptor) CD16+ (FC III receptor) cells are subset that are thought to

represent the precursors of tissue-resident macrophages and are referred to as "resident" monocytes.

Cell labeling

M1-polarized and M2-polarized macrophages were incubated with USPIO research prototype (P904, Chematech Guerbet Research, Aulnay-Sous-Bois, France) (200 µg Fe/mL) for 36 hours of the 2-day treatment with polarizing stimuli administered at 37°C in 5% CO2, basing on Chematech guidelines [28].

At least 1x106 cells per milliliter were placed in 2 mL gel phantoms made with 1.6% agarose gel.

In vitro Macrophage uptake [1]

Incubation concentration	Incubation time	THP-1 cell line
200 µgFe/mL	24 hr	1.8-2.3 pgFe/cell

Fig. 2 In vitro macrophage uptake of P904 basing on Chematech Guerbet Research

P904 is an Ultra Small Particle of Iron Oxide (USPIO) Guerbet Research Prototype designed for macrophage imaging.

P904 can be used in pre-clinical studies in several applications such as in cell labeling and trafficking, inflammation imaging, angiography and high sensitivity contrast-enhanced brain functional MRI (fMRI).

P904 has been investigated for:

· Cellular Imaging: in vitro cell labeling, cell trafficking, lymph node and liver imaging, imaging of inflammation after iv injection (atherosclerotic plaque, Alzheimer disease, multiple sclerosis, osteo-arthritis) [31-33]

· Blood pool imaging: CE-fMRI, bolus and steady state T1w-MRA, quantification of cerebral blood volume or vessel size index (VSI) [33]

The molecular characteristics of P904 are [28]:

· Hydrodynamic size: diameter is 25-30 nm

· Fe content: > 5000 Fe atoms per particle

· Recommended dose: 200 μ mol/kg = 2.5 μ L/g

Example: for a 30g body weight mouse injection, volume is 75 µL

· Relaxivities (data at 37° C; 4% Human Albumin Serum, medium closed to plasma)

B_o (T)	1.5	3.0	4.7	7.0
r1 ($s^{-1}.mM^{-1}$)	14±1	7±1	4±0.5	1.6±0.2
r2 ($s^{-1}.mM^{-1}$)	90±5	90±5	92±5	94±5

The same protocol has been followed for human cell, both for healthy volunteers M1-like and M2-like population and for patient with cholangiocarcinoma M1-like and M2-like population.

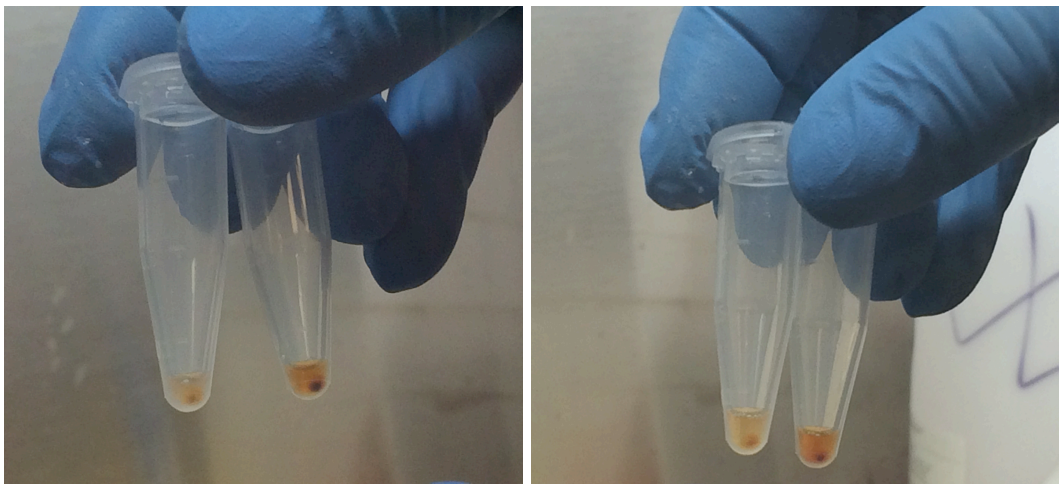

Fig.3 From the left to the right: M1-like macrophage and M2-like macrophage from the patient with cholangiocarcinoma; M1-like macrophage and M2-like macrophage from the healthy volunteer.

Evaluation of P904 cell labeling

Evaluation of P904 cell labeling with MRI

USPIO accumulation was assessed in the four TPH macrophage populations (M1-polarized macrophage plate incubated with P904; M2-polarized macrophage plate incubated with P904; control macrophage plate incubated with P904; control macrophage plate non-incubated with P904) using 3T clinical MR scanner (Discovery MR750, GE Healthcare, Milwaukee, USA).

At least 1x106 cells per milliliter were placed in 2 mL gel phantoms made with 1.6% agarose gel.

Cell phantoms were then set in the center of a transmit-receive head coil (eight-channel HRBRAIN, GE Healthcare, Milwaukee, USA) within an agarose pad.

MR scan protocol included:

- *Coronal T2* MERGE* (FOV: 24; phase FOV 0.80; SL 3.0/0.3; auto tr 938;TE 4.9; FA 2; matrix 320*224).

- *R2* mapping* was obtained using a multigradient-echo sequence, and a series of images was reconstructed at different echo times. Thirty-six gradient echoes were used to reconstruct a time series of images for R2* determination (160 millisecond [msec] repetition time, 1.9 msec interval between two uneven echoes, 30° FA, 256 × 256 spatial resolution, 2 mm section thickness, 180 mm field of view). R2 mapping was acquired using a multiecho, multisection sequence (eight echoes, 500 msec repetition time, 6.9 msec interval between two echoes, 128 × 128 spatial resolution, 2.5 mm section thickness, 180 mm field of view, 90° flip angle) [27].

- *Coronal T1 FSPGR 3D* (TR 8.1, TE 3.1, 12° flip angle, 256 × 256 spatial resolution, 1.2 mm section thickness).

The same protocol has been used for human cell labeled with P904 both for healthy volunteers M1-like and M2-like population and for patient with cholagiocarcinoma M1-like and M2-like population.

Evaluation of P904 cell labeling with Light Microscopy (LM).

In order to evaluate P904 labeling using light microscopy (Carl Zeiss Axioskop-40, Thornwood, NY, USA), the cells were cytospun (1,400 rpm for 5 minutes), and the tagged cells were collected.

Cellular USPIO uptake was confirmed by Perls' Prussian blue staining.

The cellular iron content was estimated with high power field (HPF) microscopy, and an experienced investigator, blinded to MRI data, gauged the cells for any structural changes as well as the presence and localization of intracellular iron oxide particles.

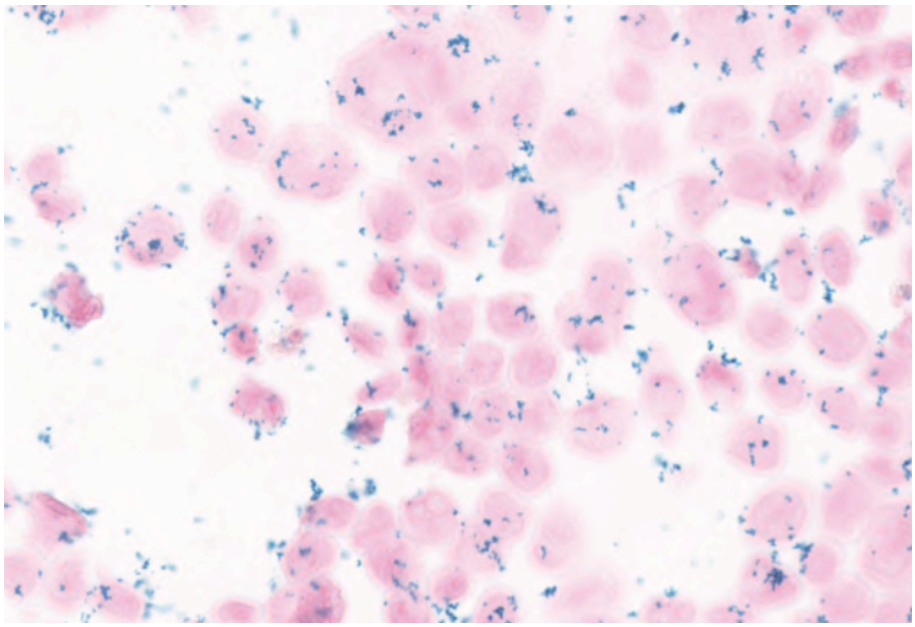

Fig.4 Cellular iron content estimated with high power field (HPF) microscopy (40x) in the M2-polarized TPH-1 macrophage plate incubated with P904

Evaluation of P904 cell labeling with Transmission Electron Microscopy (TEM).

Macrophages were detached and transferred in the Eppendorf tubes for transmission electron microscopy (TEM) processing.

After centrifugation, the cell pellet was fixed with 2.5% glutaraldehyde (SIC, Rome, Italy) in 0.1M PBS for two days at 4°C and then rinsed with PBS. Afterwards, samples were post-fixed using 1.33% osmium tetroxide (Agar Scientific, Stansted, UK) for 2 hours and rinsed again in PBS.

The specimens were dehydrated by exchange with ethanol (30%, 70%, 95%, 100% v/v x 3), immersed in propylene oxide (BDH Italia, Milan, Italy) for solvent substitution and embedded in epoxy resin Embed-812 (SIC, Rome, Italy).

Semithin (1µm) and ultrathin (80-90nm) sections were obtained using an ultramicrotome (Leica EM UC6, Vienna, Austria); for the LM analysis, the semithin sections were collected on slides and stained blue by Azur II, and imaging was performed using a light microscope (Carl Zeiss Axioskop-40, Thornwood, NY, USA).

Whereas for the TEM observation, the ultrathin sections were collected on 100-mesh copper grids (Assing, Rome, Italy) stained with a rare-earth elements solution and lead citrate. Imaging was performed using a transmission electron microscope set with an accelerating voltage of 60kV (Carl Zeiss EM10 , Thornwood, NY, USA) while images were acquired using a digital camera (AMT CCD, Deben UK Ltd, Suffolk, UK).

An experienced investigator, blinded to MRI data, gauged the cells for any structural changes as well as the presence and localization of intracellular iron oxide particles.

Data analysis

MRI data analysis

Two radiologists were blinded and MR images (considered as adequate) were

independently read.

The primary evaluation criteria included observing changes in every plate, and in particular, the presence of slope effect was appraised.

At least 10 ROI measurements for every single plate were performed for the evaluation of T1w, T2*w and R* datasets. Multisection, multiple-echo, quantitative R2* data were evaluated using FuncTool 4.5.3 (GE Healthcare, Milwaukee, USA).

LM and TEM data analysis

An experienced investigator, blinded to MRI data, gauged the cells for any structural changes as well as the presence and localization of intracellular iron oxide particles both in LM dataset and in TEM dataset.

Statistical Analysis

For each population, measurements were averaged and results reported as a mean ± standard deviation. A 95% interval of confidence (IC) was also calculated and presented. Normal distribution of the data was determined by using the Shapiro-Wilk test.

For each MRI parameter (T1, T2, R*), results among the four different populations were analyzed and compared using the repeated measurements of analysis of variance. Cellular iron content in the three populations was evaluated and compared as well by using repeated measurements of analysis of variance.

A p value < 0.05 was considered statistically significant.

All of the analyses were performed using SPSS (version 22.0, SPSS Inc, Chicago, IL, USA).

RESULTS

Human THP-1 monocytes were differentiated into macrophages by incubation in the presence of PMA. Cells became adherent and the expression of recognized macrophage markers, CD68 (cluster of differentiation 68), were analyzed by immunofluorescence staining, and based upon the literature, we polarized macrophages in M1 and M2 phenotype. Macrophage M1 and M2 polarization was confirmed by measuring the expression of classical M1 markers: iNOS for M1 and Mannose receptor 1 (Mrc1) at the mRNA level using RT-qPCR (Table 1).

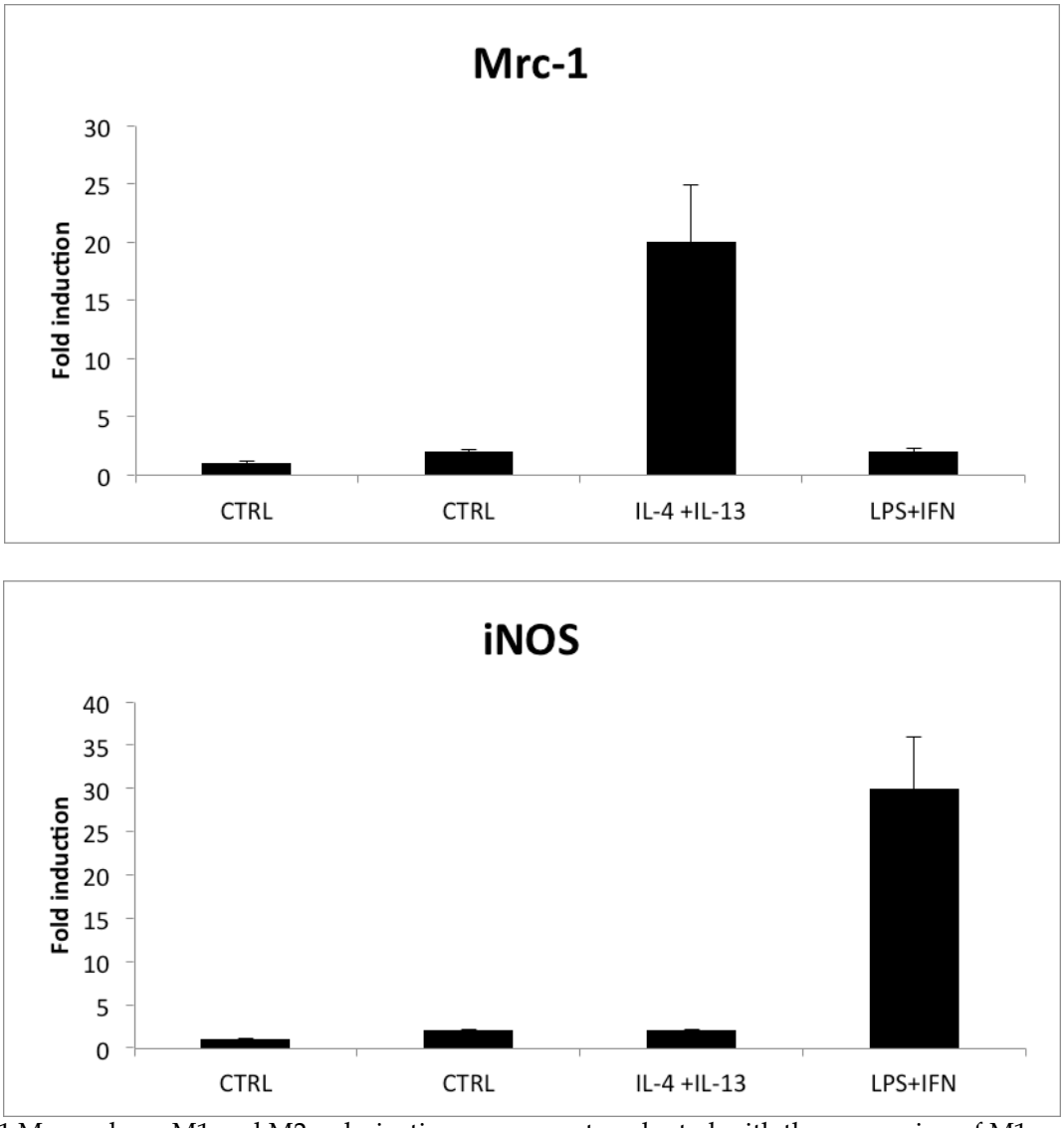

Table 1 Macrophage M1 and M2 polarization assessment evaluated with the expression of M1 markers: iNOS for M1 and Mannose receptor 1 (Mrc1) at the mRNA level using RT-qPCR .

The ***T1 signal*** for the M2-polarized population (1982.0 ± 54.2, 95% IC 1912.8-2048.1) was significantly higher compared to both the M1-polarized population (740.5 ± 32.1, 95% IC 705.5-775.4, p<0.0001) and the M0-P904 population (769.7 ± 40.0, 95% IC 743.8-795.5, p<0.0001). The T1 signal in the M0 population (411.3 ± 25, 95% IC 405.8-415.2) was significantly lower compared to all of the populations (all p<0.0001). No significant differences were observed between M1 and M0-P904 (p=0.99).

The ***T2* signal*** for the M0 population (1050.6 ± 66.1, 95% IC 1.32.7-1068.4) was significantly higher compared to the M0-P904 (919.9 ± 57.8, 95% IC 891.5-936.3, p<0.0001), M1-polarized (1004.1 ± 68.9, 95% IC 998.6-1009.5, p<0.0001) and M2-polarized populations (576.6 ± 37.6, 95% IC 565.5-587.5, p<0.0001). The T2 signal for the M2-polarized population was significantly lower compared to the other groups (all p<0.0001).

R* was significantly higher for the M2-polarized population (68.1 ± 6.0, 95% IC 64.1-72.0) compared to the other populations (all p<0.0001), while R* was significantly lower for M0 (3.7 ± 1.3, 95% IC 0.8-6.6) compared to M0-P904 (16.9 ± 3.2, 95% IC 15.4-18.7, p<0.001). No significant differences were found between the M1-polarized population (6.5 ± 3.7, 95% IC 5.4-7.5) and the M0 population (p=0.31) (Figure 5).

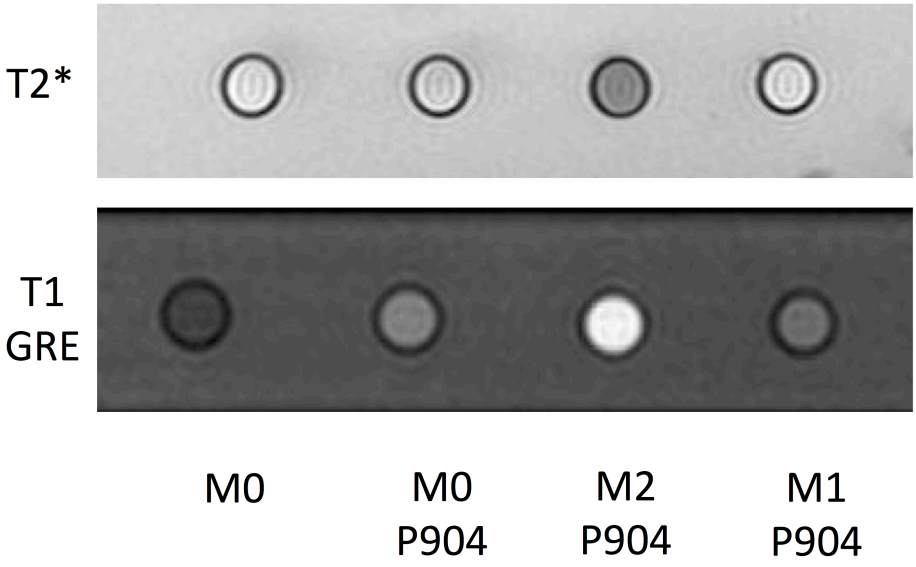

Fig5 USPIO MR. M2-polarized population showing high signal on T1 weighted images and low signal in T2*

M2 phantom demonstrated the *slope effect* after 48 hours of incubation non visible in the other populations.

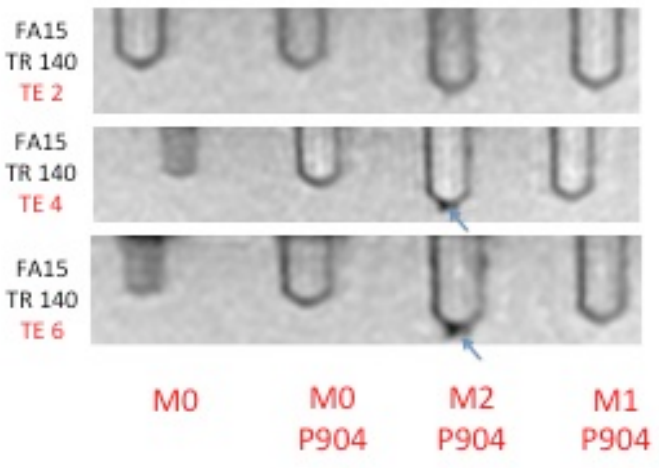

Fig 6 Slope effect has been demonstrated in the M2 polarized population and it is more noticeable when the TE is higher.

Cellular iron content was evaluated in the M1-polarized, M2-polarized and M0 P904 population.

The number of macrophages with iron content in the M2-polarized population was 32.1 ± 8.5 (95% IC 28.1-43.8) significantly higher when compared to both the M1 polarized population (20.3 ± 7.1, 95% IC 12.2-28.2, p=0.04) and the M0-P904 population (2.3 ± 1.1, 95% IC 1.0-3.6, p=0.003).

Significant differences were also observed and reported by comparing the M1-polarized population to the M0-P904 population (p=0.005).

The TEM demonstrated a ubiquitous distribution of P904 within the cellular compartments including cytoplasm, mitochondria, plasmatic/nuclear membranes and nucleolus (Figure 2).

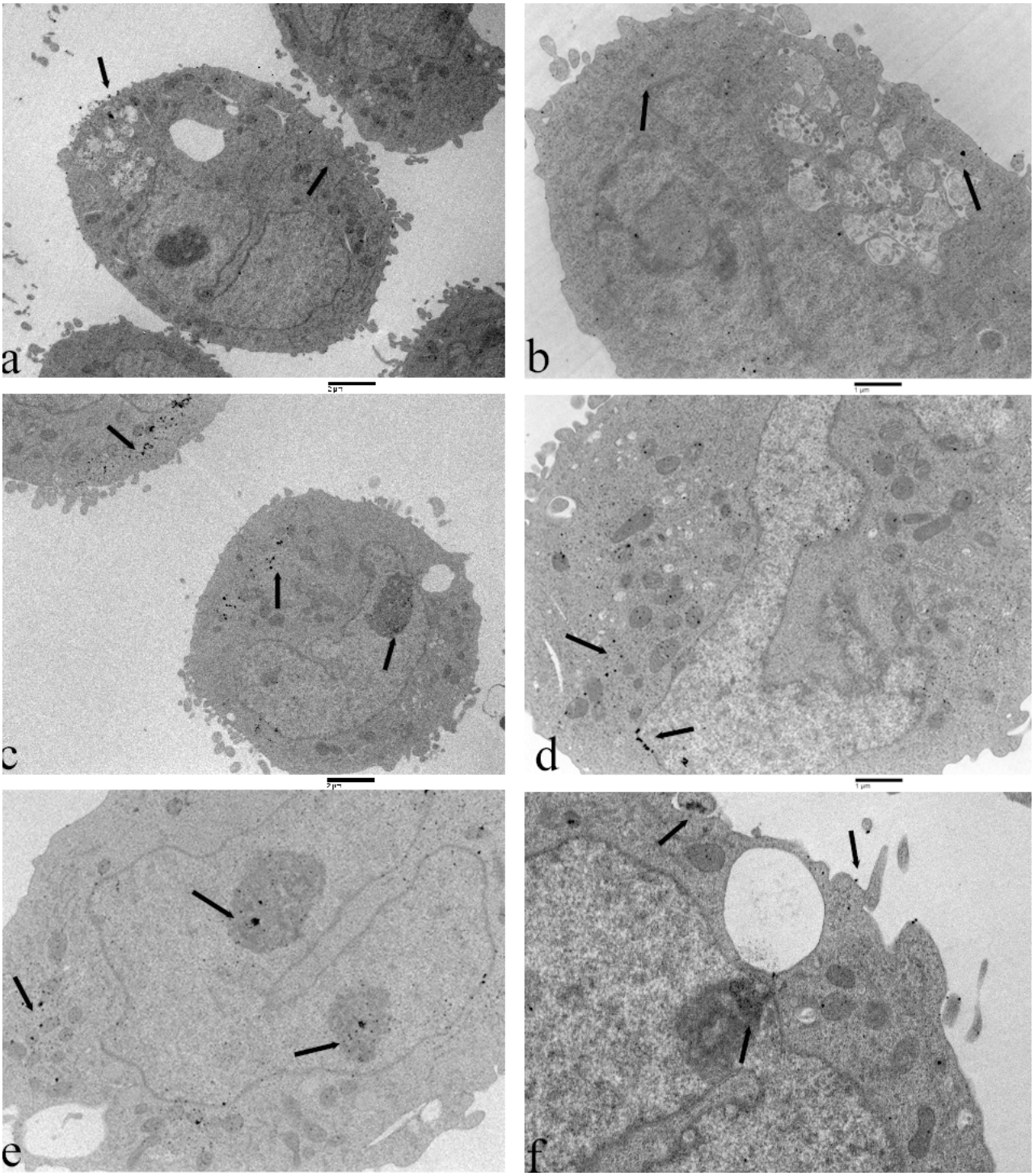

Fig 7 Transmission electron microscopy (TEM) images of Human Monocyte Macrophage THP-1 cells incubated with ferric ultrasmall supermagnetic iron oxide particles (USPIO) research prototype P904. The images show the phagocytosis of USPIO and its localization was observed in several districts (black arrows): cytoplasm [a-f], mitochondria [a, d, e], plasmatic/nuclear membranes [a, d, f], and nucleolus [e, f].

Same results were validated also in the macrophage populations derived from human cell.

	T1	T2*	R*
PZ M1 polarized+P904	**950,87 ± 203,83**	**360,84 ± 111,31**	**119,02± 25,26**
PZ M2 polarized+P904	**1514,63 ± 397,31**	**78,46 ± 18,66**	**147,97± 33,82**
HV M1 polarized+P904	**947,58 ± 261,77**	**287,13± 108,20**	**79,94 ± 34,33**
HV M2 polarized+P904	**930 ± 274,33**	**85,36 ± 25,32**	**136,99 ± 42,28**

Table 2 MRI signal of cell from patient with cholangiocarcinoma (PZ) and from healthy volunteer (HZ)

The ***T1 signal*** for the M2-polarized population from the patient with cholangiocarcinoma was significantly higher compared to both the M1-polarized population and the M2-polarized population from healthy volunteer.

The ***T2* signal*** for the M2-polarized population was significantly lower compared to the other groups in particular for M2-polarized population from the patient with cholangiocarcinoma.

R* was significantly higher for the M2-polarized population compared to the other populations.

DISCUSSION

The present study demonstrated the possibility to differentiate macrophage populations, in particular M1- and M2-polarized, based on the different labeling efficiencies, when incubated with an USPIO (P904) MR contrast agent.

After P904 incubation, T1 signal shown by M2-polarized population was significantly higher compared to the other population ($p<0.0001$), and T2* signal for M2-polarized macrophages was significantly lower compared to the other group of cells ($p<0.0001$) (Figure 1). Although R* seemed to depend on the number of labeled cells in vitro, it was significantly higher for M2 population as compared to other sub-groups ($p<0.0001$) [27].

LM confirmed MRI results as it demonstrated higher iron content in M2-polarized population compared to both M1-polarized population ($p=0.04$) and M0-P904 population ($p=0.003$). P904 particles were demonstrated to be ubiquitous in all cellular compartments, instead of the dogma of USPIO localization within the RES.

The results were confirmed using the same protocol with macrophage population derived from human PB.

These preliminary results are interesting, particularly in oncology, considering the importance of macrophages in tumor regulation, as demonstrated by many recent pre-clinical and clinical investigations [1-3]. Tumor-Associated Macrophages (TAM) originate from circulating monocytes and have a complex role in the carcinogenic process, since they participate in immune response to tumors in a polarized manner: classic M1 macrophages promote tumoricidal responses, whereas M2 macrophages, secreting growth factors that support the proliferation of neoplastic cells, delivering vascular endothelial growth factor (VEGF) to activate tumor angiogenesis, and producing cytokines and extracellular proteases, support tumor invasion and metastasis [5-7,27].

Modulation of TAM is one of the goals of the research in the attempt to skew TAM polarization into cells with a proinflammatory antitumor phenotype. Deep knowledge of the regulation of TAM functions would be essential for the development of innovative anticancer strategies [34].

As a consequence, the availability of a MR contrast medium able, in vivo, to label M2-polarized macrophages would be extremely important in assessing response to therapy. This would be crucial in the case of immunotherapy.

As it is well known from clinical practice, imaging evaluation of response to immunotherapy is difficult and late [35-36].

That the possibility of USPIO MR contrast agent are not only a dream, but a potential possibility comes from an old observation of our group, which was able to demonstrate a significant decrease of signal intensity of myometrium and cervical stroma of the uterus after USPIO particles administration in a group of patients affected by uterine cancers [25]. At that time we were unable to correlate this finding with the presence of TAM and on the basis of knowledge about pharmacological properties of the USPIO agent we were unable to provide a definite explanation of this phenomenon [37]. In fact, no macrophages are normally present within myometrium or cervical stroma, being able to uptake the contrast medium and to determine a decrease of signal intensity of both the tissues.

The absence of macrophages within cervical stroma and myometrium was also confirmed by a re-evaluation of pathologic specimens available in our cases. Thus, we focused our attention only on the radiological benefits of better conspicuity of the lesion and consequently better local staging.

In the light of today's knowledge, that was the first observation of labeled TAM, although if they were M2-polarized macrophages only is still unknown.

CONCLUSION

In conclusion, selective USPIO labeling was successfully demonstrated in the M2-polarized population.

The added value of the research is that it was conducted using a clinical 3.0T MR scanner, making further studies available for larger groups of researchers.

Further studies on same topic would be highly desirable to investigate the possible role of non-invasive diagnosis in inflammation and cancer imaging, basing on different USPIO labeling - and involvement - of M1 and M2 population.

REFERENCES

[1] Candido J et al. Cancer-related inflammation. J Clin Immunol. 2013 Jan;33 Suppl 1:S79-84.

[2] Finn OJ. Immuno-oncology: understanding the function and dysfunction of the immune system in cancer. Ann Oncol. 2012 Sep;23 Suppl 8:viii6-9.

[3] Siveen KS et al Role of macrophages in tumour progression. Immunol Lett. 2009 Apr 27;123(2):97-102.

[4] Mantovani A et al. Tumour immunity: effector response to tumour and role of the microenvironment. Lancet. 2008 Mar 1;371(9614):771-83.

[5] Riabov V et al Role of tumor associated macrophages in tumor angiogenesis and lymphangiogenesis. Front Physiol. 2014 Mar 5;5:75. eCollection 2014.

[6] Galdiero MR et al. Tumor associated macrophages and neutrophils in cancer. Immunobiology. 2013 Nov;218(11):1402-10.

[7] Biswas SK et al. Tumor-associated macrophages: functional diversity, clinical significance, and open questions. Semin Immunopathol. 2013 Sep;35(5):585-600.

[8] Capece D et al. The inflammatory microenvironment in hepatocellular carcinoma: a pivotal role for tumor-associated macrophages. Biomed Res Int. 2013;2013:187204.

[9] Ohno S et al. Role of tumor-associated macrophage in malignant tumors: should the location of the infiltrated macrophages be taken into account during evaluation? Anticancer Res. 2002 Nov-Dec;22(6C):4269-75.

[10] Mantovani A et al The origin and function of tumor-associated macrophages. Immunol Today. 1992 Jul;13(7):265-70. Review.

[11] Qian BZ et al Macrophage diversity enhances tumor progression and metastasis. Cell. 2010 Apr 2;141(1):39-51.

[12] Rolny C et al. HRG inhibits tumor growth and metastasis by inducing macrophage polarization and vessel normalization through downregulation of PlGF. Cancer Cell. 2011 Jan 18;19(1):31-44.

[13] Forssell J et al. High macrophage infiltration along the tumor front correlates with improved survival in colon cancer. Clin Cancer Res. 2007 Mar 1;13(5):1472-9.

[14] Galarneau H et al. Increased glioma growth in mice depleted of macrophages. Cancer Res. 2007 Sep 15;67(18):8874-81.

[15] Ong RM et al. Cytotoxicity of accelerated white MTA and Malaysian white Portland cement on stem cells from human exfoliated deciduous teeth (SHED): An in vitro study. Singapore Dent J. 2012 Dec;33(1):19-23.

[16] Sica A et al. Macrophage plasticity and polarization: in vivo veritas. J Clin Invest. 2012 Mar 1;122(3):787-95.

[17] Venneri MA et al. Identification of proangiogenic TIE2-expressing monocytes (TEMs) in human peripheral blood and cancer. Blood. 2007 Jun 15;109(12):5276-85.

[18] Lewis JS et al. Radiometal-labeled somatostatin analogs for applications in cancer imaging and therapy. Methods Mol Biol. 2007;386:227-40.

[19] Matsubara D et al. Lung cancer with loss of BRG1/BRM, shows epithelial mesenchymal transition phenotype and distinct histologic and genetic features. Cancer Sci. 2013 Feb;104(2):266-73.

[20] Huang B et al. The expression and role of protein kinase C (PKC) epsilon in clear cell renal cell carcinoma. J Exp Clin Cancer Res. 2011 Sep 28;30:88.

[21] Frankenberger M et al. A defect of CD16-positive monocytes can occur without disease. Immunobiology. 2013 Feb;218(2):169-74.

[22] Kim OH et al. Proangiogenic TIE2(+)/CD31 (+) macrophages are the predominant population of tumor-associated macrophages infiltrating metastatic lymph nodes. Mol Cells. 2013 Nov;36(5):432-8.

[23] Bellin MF et al. Iron oxide-enhanced MR lymphography: initial experience. Eur J Radiol. 2000 Jun;34(3):257-64.

[24] Petersein Jet al. Liver. II: Iron oxide-based reticuloendothelial contrast agents for MR imaging. Clinical review. Magn Reson Imaging Clin N Am. 1996 Feb;4(1):53-60.

[25] Laghi A et al. Decrease of signal intensity of myometrium and cervical stroma after ultrasmall superparamagnetic iron oxide (USPIO) particles administration: an MR finding with potential benefits in T staging of uterine neoplasms. Invest Radiol. 2004 Nov;39(11):666-70.

[26] Tjiu JW et al. Tumor-associated macrophage-induced invasion and angiogenesis of human basal cell carcinoma cells by cyclooxygenase-2 induction. J Invest Dermatol. 2009 Apr;129(4):1016-25.

[27] Wang Q, Li K, Quan Q, Zhang G. R2* and R2 mapping for quantifying recruitment of superparamagnetic iron oxide-tagged endothelial progenitor cells to injured liver: tracking in vitro and in vivo. Int J Nanomedicine. 2014 Apr 11;9:1815-22. doi: 10.2147/IJN.S58269. eCollection 2014.

[28] Chematech brochure available at http://www.chematech-mdt.com/uploads/Preclinical%20MRI%20probes.pdf

[29] Kinner S et al. Contrast-enhanced magnetic resonance angiography in rabbits: evaluation of the gadolinium-based agent p846 and the iron-based blood pool agent p904

in comparison with gadoterate meglumine. Invest Radiol. 2011 Aug;46(8):524-9. doi: 10.1097/RLI.0b013e31821ae21f.

[30] Kinner S et al. Comparison of two different iron oxide-based contrast agents for discrimination of benign and malignant lymph nodes. Invest Radiol. 2012 Sep;47(9):511-5. doi: 10.1097/RLI.0b013e3182587744.

[31] Sigovan M et al. Rapid-clearance iron nanoparticles for inflammation imaging of atherosclerotic plaque: initial experience in animal model. Radiology. 2009 Aug;252(2):401-9. doi: 10.1148/radiol.2522081484.

[32] López-Castro JD et al. From synthetic to natural nanoparticles: monitoring the biodegradation of SPIO (P904) into ferritin by electron microscopy. Nanoscale. 2011 Nov;3(11):4597-9. doi: 10.1039/c1nr10980d. Epub 2011 Oct 11.

[33] Luciani A et al. Adipose tissue macrophages: MR tracking to monitor obesity-associated inflammation. Radiology. 2012 Jun;263(3):786-93. doi: 10.1148/radiol.12111957. Epub 2012 Apr 20.

[34] Danella Polli C et al Jacalin-Activated Macrophages Exhibit an Antitumor Phenotype. Biomed Res Int. 2016;2016:2925657. doi: 10.1155/2016/2925657. Epub 2016 Mar 29.

[35] Kwak JJ, Tirumani SH, Van den Abbeele AD, Koo PJ, Jacene HA. Cancer immunotherapy: imaging assessment of novel treatment response patterns and immune-related adverse events. Radiographics. 2015 Mar-Apr;35(2):424-37. doi: 10.1148/rg.352140121.

[36] Juergens RA, Zukotynski KA, Singnurkar A, Snider DP, Valliant JF, Gulenchyn KY. Imaging Biomarkers in Immunotherapy. Biomark Cancer. 2016 Feb 25;8(Suppl 2):1-13. doi: 10.4137/BIC.S31805. eCollection 2016.

[37] Korchinski DJ, Taha M, Yang R, Nathoo N, Dunn JF. Iron Oxide as an MRI Contrast Agent for Cell Tracking. Magn Reson Insights. 2015 Oct 6;8(Suppl 1):15-29. doi: 10.4137/MRI.S23557. eCollection 2015.

The present work or part of it has been presented at

- *ECR 2016 European Society of Radiology Annual Congress*; 2-10 March 2016,Vienna, Austria

USPIO-labeling in M1 and M2 macrophage population: an in vitro MR study.

C.Zini, M. Venneri, M. Rengo, N. Porta, A. Isidori, V. Petrozza, A. Laghi.

- *ISMRM-Italian Chapter*- Bologna, Italy; 4-5 February 2016

USPIO-labeling in different macrophage population: an in vitro MR study

C.Zini, M. Venneri, M. Rengo, D.Caruso, N. Porta, A. Isidori, V. Petrozza, A. Laghi.

- *ESOI Annual Meeting* -Turin, Italy; 10- 12 September 2015

USPIO-labeling in different macrophage populations: an *in vitro* study using a 3.0T clinical scan

C Zini, M Venneri, M Rengo, N Porta, A Isidori, V Petrozza, A Laghi.

The present work will be presented at

- *RSNA 2016 - 102nd Scientific Assembly and Annual Meeting of Radiology Society of North America*; 27 November - 5 December 2016, Chicago, U.S.A

USPIO-labeling in different macrophage population: an in vitro and in vivo MR study.

C Zini, MD, ;M Venneri ;D Caruso, MD; S Miglietta; M Rengo, MD; N Porta,MD; A Isidori, MD; V Petrozza, MD; A Laghi, MD.

The present work has been summited for a possible publication to *Oncotarget-Impact Journal*.